JOURNAL OF MATERIALS SCIENCE 19 (1984) 2795–2804

Transmission electron microscopic observations of a commercial Nb–Ti superconducting alloy

S. HANADA, A. NAGATA, S. DEN, O. IZUMI
The Research Institute for Iron, Steel and Other Metals, Tohoku University, Sendai 980, Japan

Microstructures in a commercial Nb–Ti alloy heat-treated or repeatedly aged and cold worked have been investigated by transmission electron microscopy. In the aged samples after solution treatment, ω-phase forms at ageing temperatures below 673 K and α-phase precipitates at 773 K. Cold work after solution treatment or heavy cold work without prior solution treatment results in accelerated precipitation of ω-phase on ageing at 623 K and of α-phase on ageing at 773 K, while it gives α-precipitation instead of ω on ageing at 673 K. Repeated ageing and cold work make the microstructures very fine. The refinement is due to formation of dislocation cell structures and subgrains and precipitation of ω- and α-phases.

1. Introduction

The NbTi alloys are used commercially as superconducting materials because of their good ductility and compatibility with copper. The critical current density (J_c) of NbTi alloys has been investigated extensively as a function of composition, cold work and heat-treatments [1–8]. Recently, J_c in high magnetic fields was found to be improved by suitable processing conditions, such as cyclically repeating heat-treatment and cold work. It is not easy, however, to identify the precipitates in the so-treated NbTi alloys, since the microstructures after heavy cold-working are very fine and complicated. However, the precipitates may be estimated in the alloys from the observation of microstructures using slightly cold worked specimens.

A few investigations [9–14] have been reported on the effect of metallurgical factors on the microstructures of the alloys. However, they were concerned with observations under restricted ageing conditions. The present work aims to investigate microstructures in detail under various heat-treatments after solution treatment and cold work.

2. Experimental procedure

The material used in this study is a commercial Nb–50 mass% Ti alloy of 16 mm diameter supplied from Furukawa Metals Co, Ltd. The composition of this alloy is 51.7 mass% niobium (25.6 mol% niobium) with impurities of 120 mass ppm carbon, 570 mass ppm oxygen, 110 mass ppm nitrogen and 10 mass ppm hydrogen. The rod was cold forged and rolled to a plate 0.5 mm thick. Part of the plate was further cold rolled to a plate 0.1 mm thick, solution treated at 1173 K for 18×10^3 sec under a vacuum of less than 3×10^{-3} Pa and then aged at various ageing conditions. Repeated heat-treatment and cold work were conducted using the starting materials at the 0.5 mm thick plate. Transmission electron microscopic observations were performed by a 200 kV EM (JEM200B).

3. Results and discussion

3.1. Ageing after solution treatment

Thin foil of the as-solution treated Nb–Ti showed neither athermal ω-phase nor martensite to be present, as only diffused lines of intensity in addition to β-reflections were observed in a selected-area diffraction pattern.

Ageing the solution treated Nb–Ti at 573 K for 3.6×10^6 sec results in a uniform dispersion of small ω-phase particles. Fig. 1a shows a dark-field micrograph containing the corresponding $\langle 1\,1\,0 \rangle_\beta$ diffraction pattern, and Fig. 1b is a schematic

0022–2461/84 $03.00 + .12

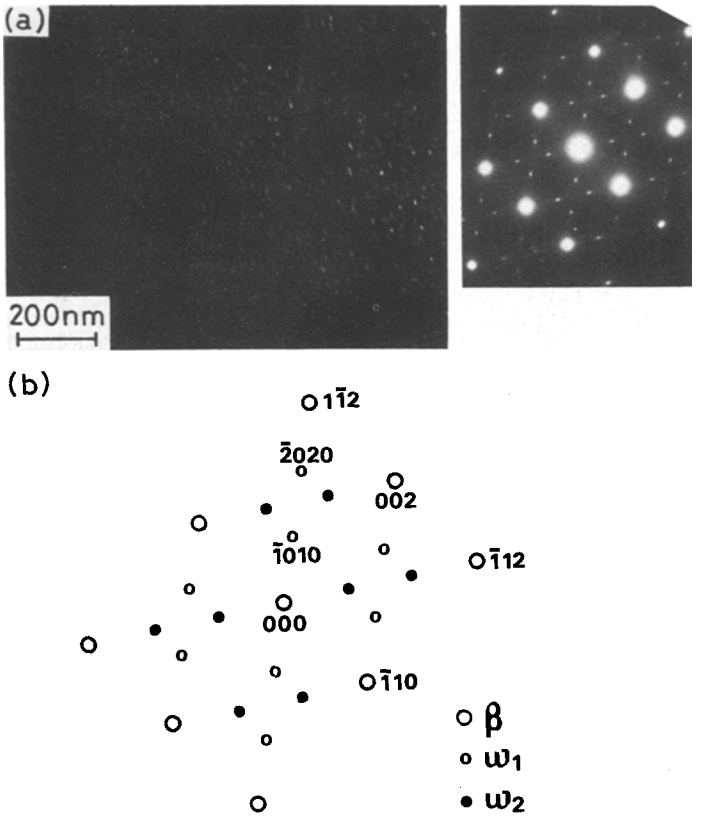

Figure 1 (a) Dark-field micrograph and electron diffraction pattern of NbTi aged at 573 K for 3.6×10^6 sec after solution treatment. (b) $\langle 1\,1\,0 \rangle_\beta$ zone pattern of (a).

representation of the pattern. Particles are seen in a $\langle 1\,1\,1 \rangle$ row. The $\langle 1\,1\,1 \rangle$ row morphology of ω-phase particles has been observed in many β-Ti alloys. Fig. 2 shows a bright-field micrograph with the mottled contrast of Nb–Ti aged at 623 K for 3.6×10^3 sec. ω-reflections are visible in the $\langle 1\,1\,0 \rangle_\beta$ electron diffraction pattern. As shown in Fig. 3a, although decomposition seems to occur in a bright-field image of Nb–Ti aged at 673 K for 3.6×10^3 sec, reflections of the precipitated phase are invisible in the diffraction pattern. A pair of dark segments with a line of zero intensity are also seen in this figure. The occurrence of contrast has been discussed by Sudareva *et al.* [15] in terms of coherency strain around particles. With continued ageing, the ω-phase is clearly observed in a $\langle 1\,1\,1 \rangle$ row morphology, Fig. 3b. Thus, it is apparent that the ω-phase precipitates on ageing at temperatures below 673 K. ω-phase precipitation in the alloy with lower titanium content is not surprising. Recently, the phase boundary in the Nb–Ti system was estimated by Larbalestier [16] based on many extensive data, showing that the $\beta/\alpha + \beta$ boundary exists above 773 K, even in the composition of Nb–65 mol% Ti. Therefore, commercial superconducting Nb–Ti alloys of a single β-phase are metastable between room temperature and 773 K. However, two different observations have been reported on the decomposition of Ti–30 to 40 mol% Nb alloys aged at low temperatures. Ishida *et al.* [9] and Osamura *et al.* [10] observed ω-phase precipitation by transmission electron microscopy in the Nb–60 mol% Ti aged at 623 K and Nb–64 mol% Ti aged at 653 K. On the other hand, Hickman [17] could not detect ω-phase precipitation by the X-ray diffraction method in Nb–65 and 70 mol% Ti alloys. Although this discrepancy cannot be explained consistently, it may be due to the fact that ω-phase precipitation is remarkably suppressed by increasing the solute content or impurities, such as oxygen or nitrogen [18–20].

When Nb–Ti is aged at 773 K, discs lying in $\{1\,0\,0\}_\beta$ planes appear at short ageing times and characteristic contrasts arising from coherency strains around the discs are seen, as shown in Fig. 4a. However, the quantity of discs is insufficient to obtain clear diffraction patterns for phase identification. After ageing at 773 K for 3.6×10^6 sec, plate-like precipitates are densely present (Fig. 4b). They are determined to be Burgers orientated α-phase particles (Fig. 4c).

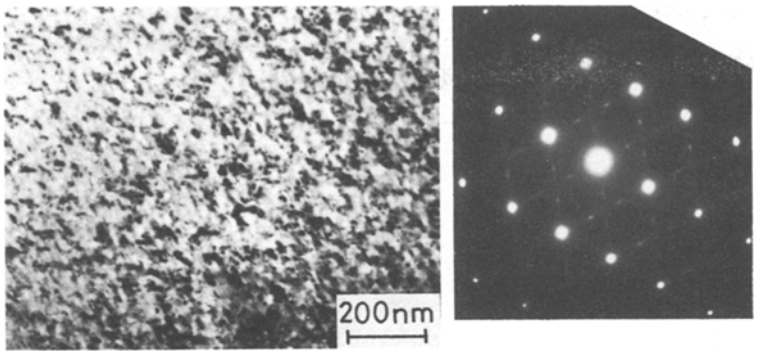

Figure 2 Bright-field micrograph and electron diffraction pattern of NbTi aged at 623 K for 3.6×10^6 sec after solution treatment.

3.2. Ageing after solution treatment followed by cold work

Figs. 5a and b are dark-field micrographs of Nb–Ti aged at 623 K for 1.8×10^6 sec after 10% and 40% cold work in reduction, respectively. Sharp ω-reflections are seen in the figures. When the Nb–Ti is not subjected to cold work, ω-reflections of the solution treated Nb–Ti become clear on ageing at 623 K for more than 3.6×10^6 sec, as shown in Fig. 2. Only diffuse lines of intensity were observed on ageing under the same conditions as that of Fig. 5. Therefore, it is concluded that cold work accelerates the precipitation of the ω-phase. Fig. 6a shows a $\langle 1\,0\,0 \rangle_\beta$ diffraction pattern of Nb–Ti aged at 673 K for 72×10^3 sec after 10% cold work, which is the same pattern as that of Fig. 4b, although the relative intensities of the α-reflection to β are different. Fig. 6b is a $\langle 1\,1\,1 \rangle_\beta$ diffraction pattern of Nb–Ti aged at 673 K for 72×10^4 sec after 10% cold work; a schematic representation of Fig. 6b is shown in Fig. 6c, indicating Burgers orientated α-phase formation. Fig. 6 is in marked contrast to Fig. 3, where ageing products are ω precipitates. Thus, on ageing at 673 K, cold work suppresses ω-phase precipitation and instead accelerates α-phase precipitation. This result suggests that ω-phase is metastable and changes to α-phase on prolonged ageing.

Fig. 7a shows a bright-field micrograph of Nb–Ti aged at 773 K for 72×10^3 sec after 10% cold work. The size of the plate-like particles is

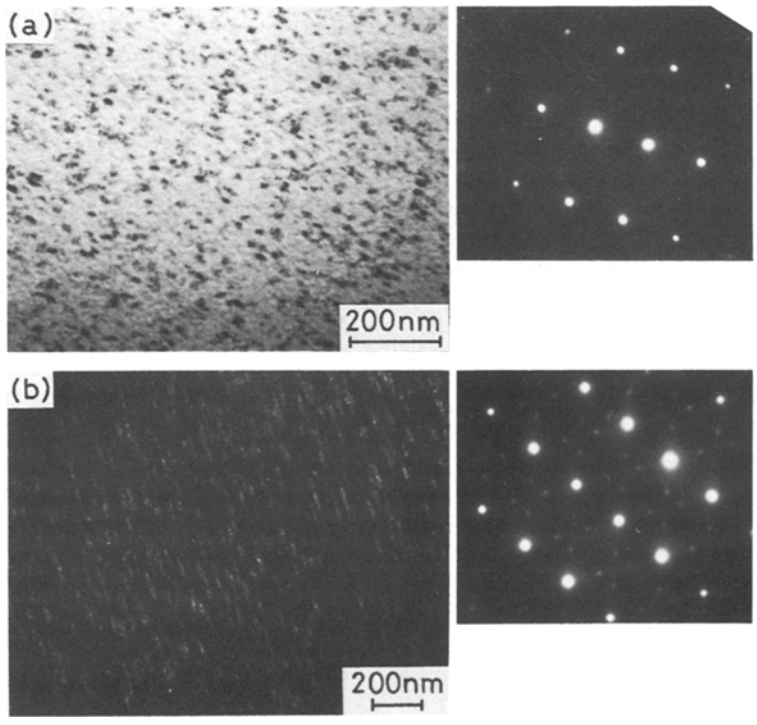

Figure 3 (a) Bright-field micrograph and electron diffraction pattern of NbTi aged at 673 K for 3.6×10^3 sec. (b) Dark-field micrograph and electron diffraction pattern of NbTi aged at 673 K for 1.8×10^6 sec.

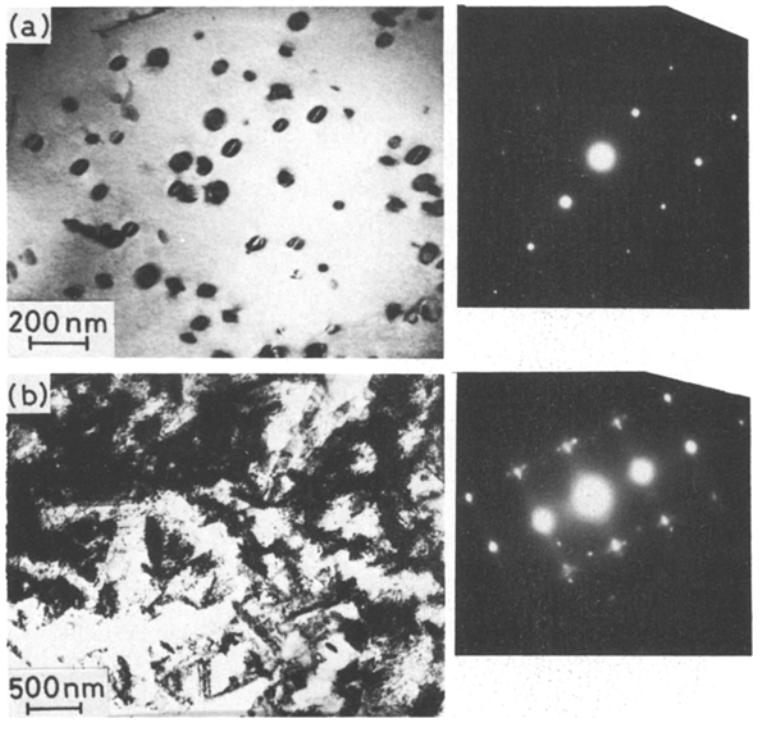

Figure 4 Bright-field micrograph and electron diffraction pattern of NbTi aged at 773 K for (a) 72×10^3 sec; and (b) 3.6×10^6 sec. (c) $\langle 0\,0\,1 \rangle_\beta$ zone pattern of (b).

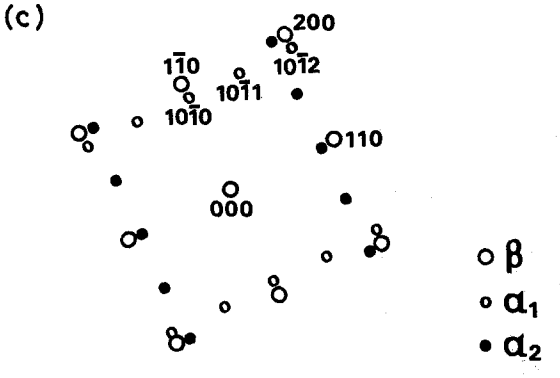

larger than those in Fig. 4a in spite of the same ageing conditions. Although extra weak spots are observed, phase identification is impossible. Figs. 7a and c show bright-field micrographs of Nb–Ti aged at 773 K for 72×10^3 sec after 40% cold work. The particles are always present along with tangled dislocations or dislocation networks. In comparison with Fig. 4a, it is apparent that α-phase precipitation is accelerated by cold work. Two Burgers orientated α_1- and α_2-reflections are seen in the diffraction pattern of Fig. 7b. However, several reflections in the pattern are not identified as α_1 or α_2. The α-phase which does not obey a Burgers orientation relationship, denoted "Type 2α" or non-Burgers α, has been observed in many β-Ti alloys, e.g. Ti–12Mo [21], Ti–14Mo–6Al [21], Ti–3Al–8V–6Cr–4Zr–4Mo [22–24], Ti–15Mo–5Zr [25] and Ti–10V–2Fe–3Al [26]. Therefore, several reflections, not identified as α_1 and α_2 in the diffraction pattern of Fig. 7b, seem to belong to the so-called type 2α. The cause for the occurrence of type 2α is not clearly understood at present. Rhodes and Williams' [21] interpretation is that type 2α is in a $\{1\,0\,\bar{1}\,2\}\langle 1\,0\,\bar{1}\,1 \rangle$ twin orientation with respect to Burgers orientated α. On the other hand, Morgan and Hammond [24] have identified type 2α as fcc. Accordingly, further study will be required on type 2α in Nb–Ti alloys. The present investigation verifies that cold work tends to promote precipitation of both ω and α. The results suggest that defects introduced by cold work serve as nucleation sites and accelerate compositional change in the ω- and α-precipitation.

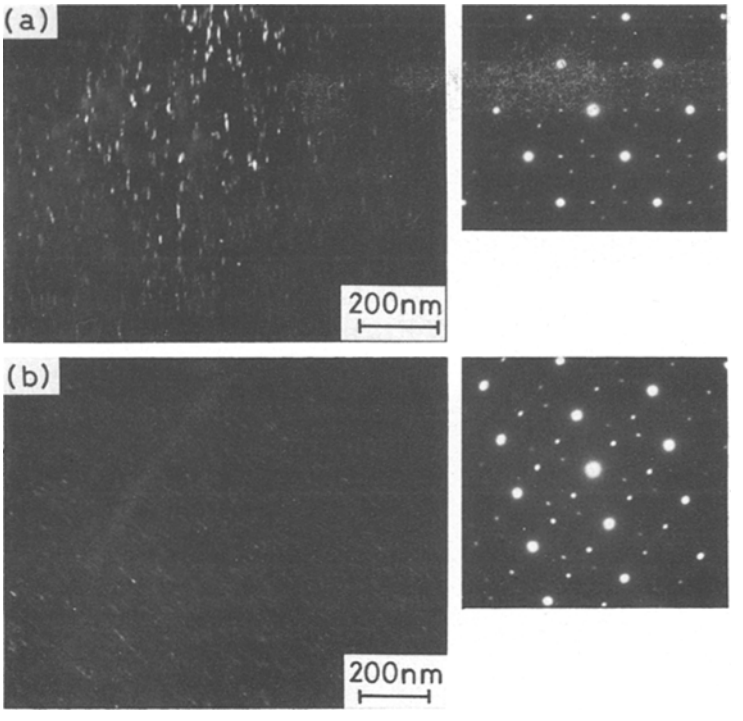

Figure 5 Dark-field micrograph and electron diffraction pattern of NbTi aged at 623 K for 1.8 × 10^6 sec after solution treatment followed by (a) 10% cold work, and (b) 40% cold work.

3.3. Ageing after heavy cold work without prior solution treatment

Ageing at 623 K after heavy cold work without prior solution treatment results in a mixed structure of deformation and recrystallization. ω-phase is often observed to form in regions with a low dislocation density (Figs. 8a and b). ω-phase also forms on ageing at 573 K (Fig. 8c). By comparing Fig. 8 with Figs. 1 and 2, it is confirmed that strain from heavy cold work favours ω-phase precipitation. Ageing at 673 K gives blocky α-precipitates and unidentified fine particles, as well as recovered or recrystallized structures (Fig. 9). Recrystallization develops at an initial stage of ageing at 773 K and with continued ageing the material is filled up by recrystallized grains (Fig. 10). Blocky

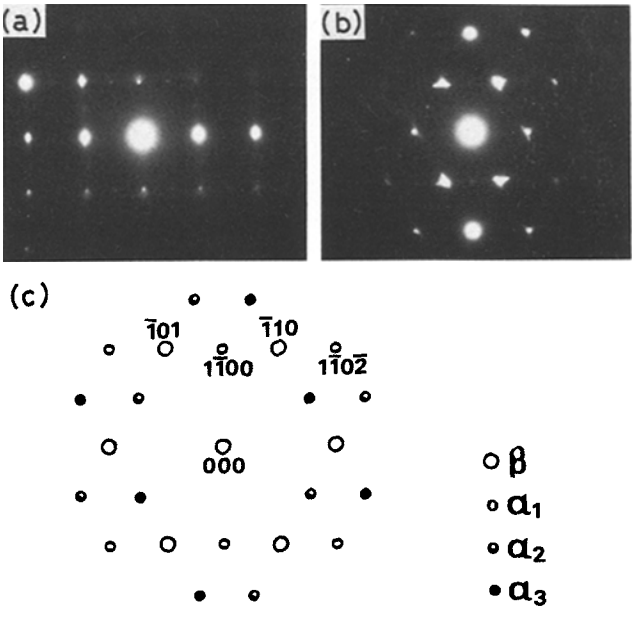

Figure 6 Electron diffraction pattern of NbTi aged at 673 K for (a) 72 × 10^3 sec, and (b) 720 × 10^3 sec after solution treatment followed by 10% cold work. (c) $\langle 1\,1\,1\rangle_\beta$ zone pattern of (b).

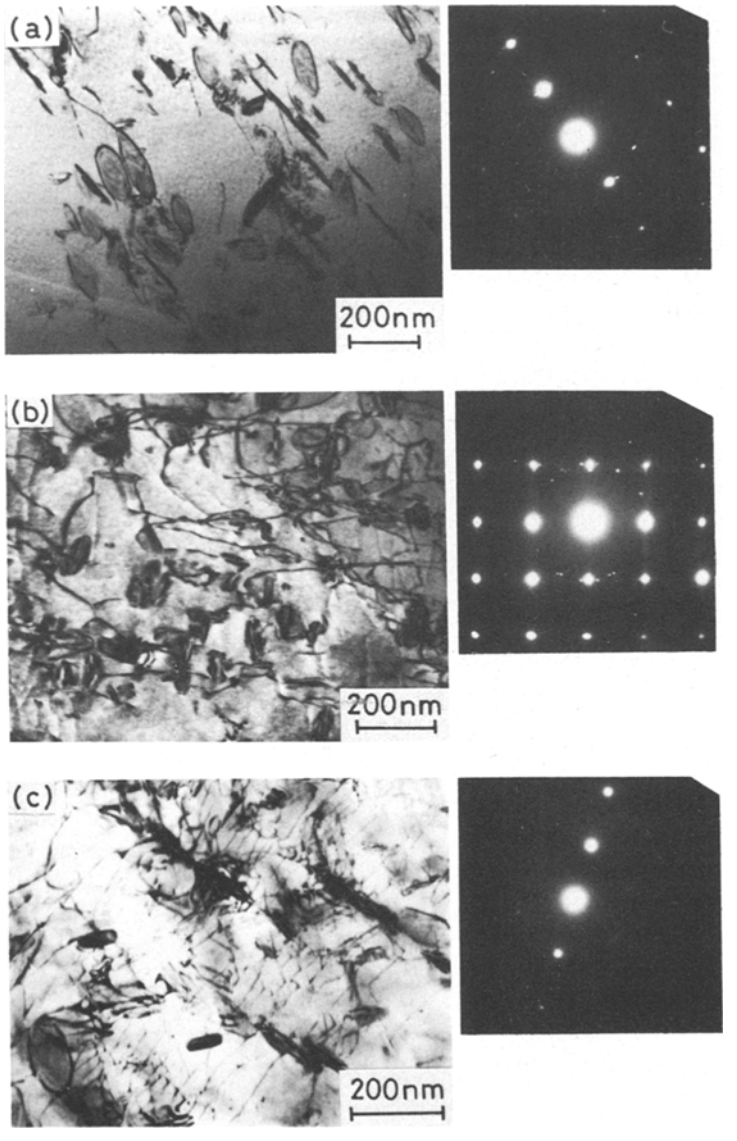

Figure 7 Bright-field micrograph and electron diffraction pattern of NbTi aged at 773 K for 72×10^3 sec after solution treatment followed by (a) 10% cold work, and (b), (c) 40% cold work.

α-precipitates are frequently observed. Therefore, heavy cold work promotes α-precipitation as well as ω-precipitation.

3.4. Repeated ageing and cold work

Repeated ageing and cold work applied to the starting material of the 0.5 mm thick plate will be expressed by sequence of AWAW. . ., where A and W indicate ageing and cold-working treatment, respectively. All the samples were cold rolled to 0.1 mm thick by the final work W in the sequence. Fig. 11a is a bright-field micrograph of the AW sample (ageing condition of A: at 623 K for 173×10^3 sec). Sub-bands are not present, but faintly delineated cell boundaries composed of tangled dislocations with a high density are observed. Fig. 11b shows subgrains which appeared in the AWA sample. In another region of the foil, dislocation cell structures remained, as they were present before the final ageing. Fig. 11c shows deformation microstructure in the AWAW sample, indicating the formation of a fine cell structure produced by working the material with fine subgrain structure. The dislocation cell structure seems to be more clearly delineated than that of Fig. 11a. ω-phase precipitation was occasionally detected in an aged sample. Fig. 11d is an example in the AWAWA sample. Therefore, the sample of Fig. 11c seems to contain fine ω-precipitates even when they are not identified by an electron dif-

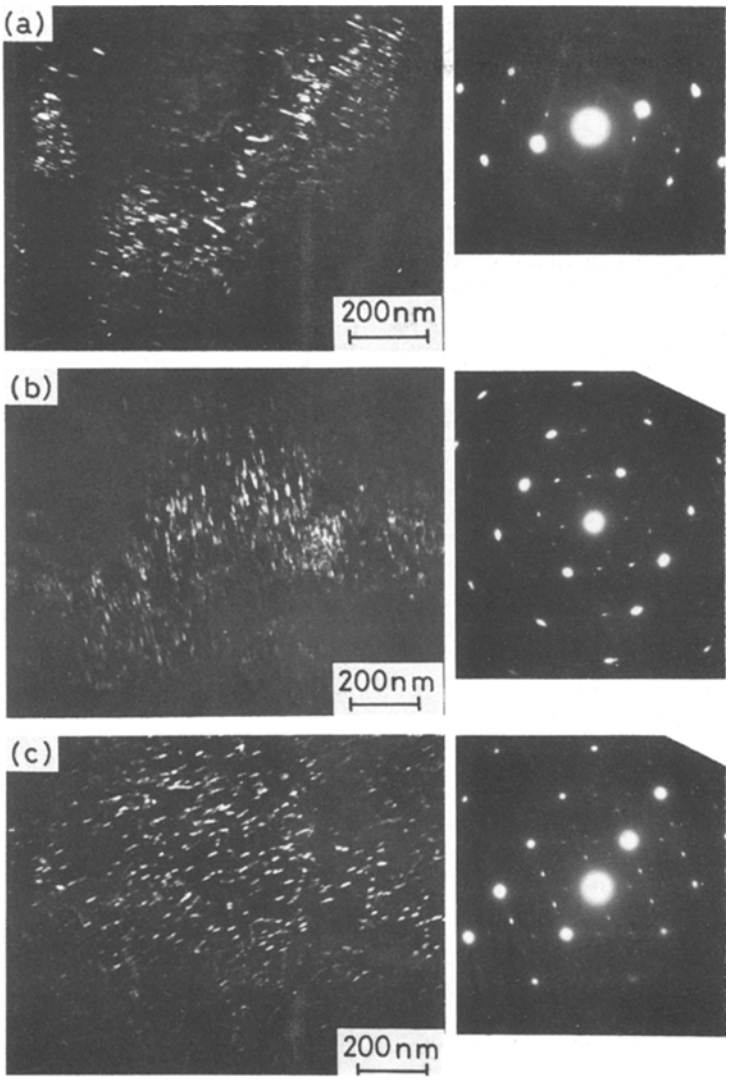

Figure 8 Dark-field micrograph and electron diffraction pattern of NbTi aged at 623 K for (a) 180×10^3 sec, (b) 3.6×10^6 sec, and (c) aged at 573 K for 720×10^3 sec after heavy cold work.

fraction pattern. Fig. 12a shows a bright-field micrograph of the AW sample (ageing condition of A: at 673 K for 3.6×10^3 sec), where tangled dislocations are distributed inhomogeneously. Fine subgrains and partially rearranged dislocation structures co-exist in the AWA sample (Fig. 12b). Fig. 12c shows dislocation cell structures observed in the AWAW sample. Compared with Fig. 12a, repeated ageing and cold work result in fine dislocation cell structures. Fig. 12d shows fine subgrains and rearranged dislocations in the AWAWA sample. Although precipitates were not identified in these sample, Fig. 9 suggests that fine α-precipitates may be formed.

As a result, repeated ageing and cold work make the microstructures very fine, since dislocation cell structures, subgrains and/or precipitates form depending upon the condition of repeated treatment. Nagata *et al.* [27] reported that the repeated treatments improve J_c of this alloy in a high magnetic field, especially in the AW . . . W sample compared with in the AW . . . A sample. This result suggests that dislocation cell structures introduced by the final cold work raise J_c more effectively than do subgrains formed by the final ageing.

4. Conclusion

Detailed observations using transmission electron microscopy have revealed transformation products and microstructures in a commercial Nb–Ti alloy heat-treated or repeatedly aged and cold worked.

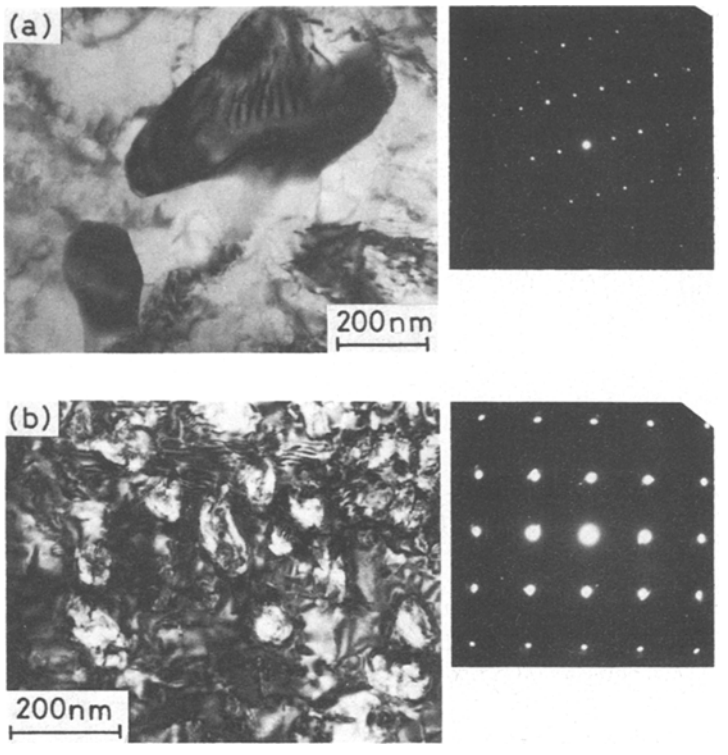

Figure 9 Bright-field micrograph and electron diffraction pattern of NbTi aged at 673 K for (a) 72×10^3 sec and (b) 72×10^4 sec after heavy cold work.

1. In the aged samples after solution treatment, ω-phase forms at ageing temperatures below 673 K and α-phase precipitates at 773 K.

2. Cold work after solution treatment or heavy cold work without prior solution treatment results in accelerated precipitation of ω-phase on ageing at 623 K and of α-phase on ageing at 773 K, while it gives α-precipitation instead of ω on ageing at 673 K.

3. Repeated ageing and cold work make the microstructures very fine. The refinement is due to formation of dislocation cell structures and subgrains and precipitation of ω- and α-phases.

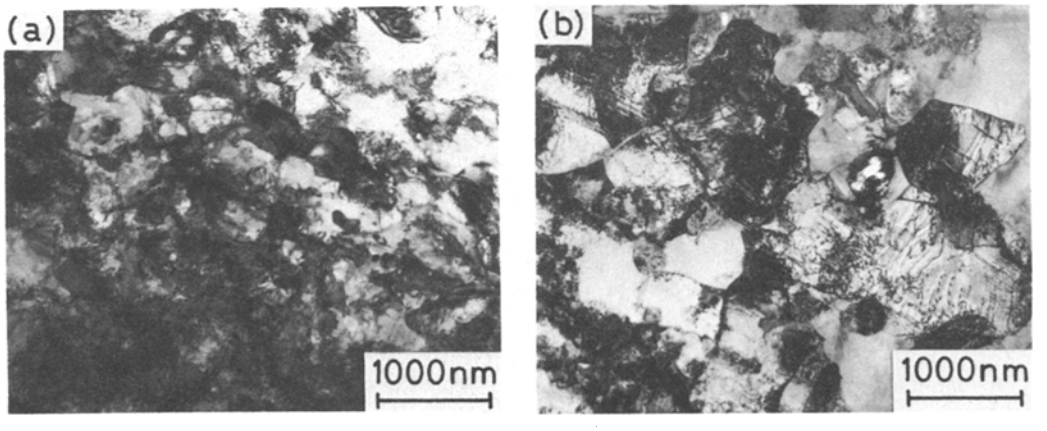

Figure 10 Bright-field micrograph of NbTi aged at 773 K for (a) 3.6×10^3 sec and (b) 36×10^4 sec after heavy cold work.

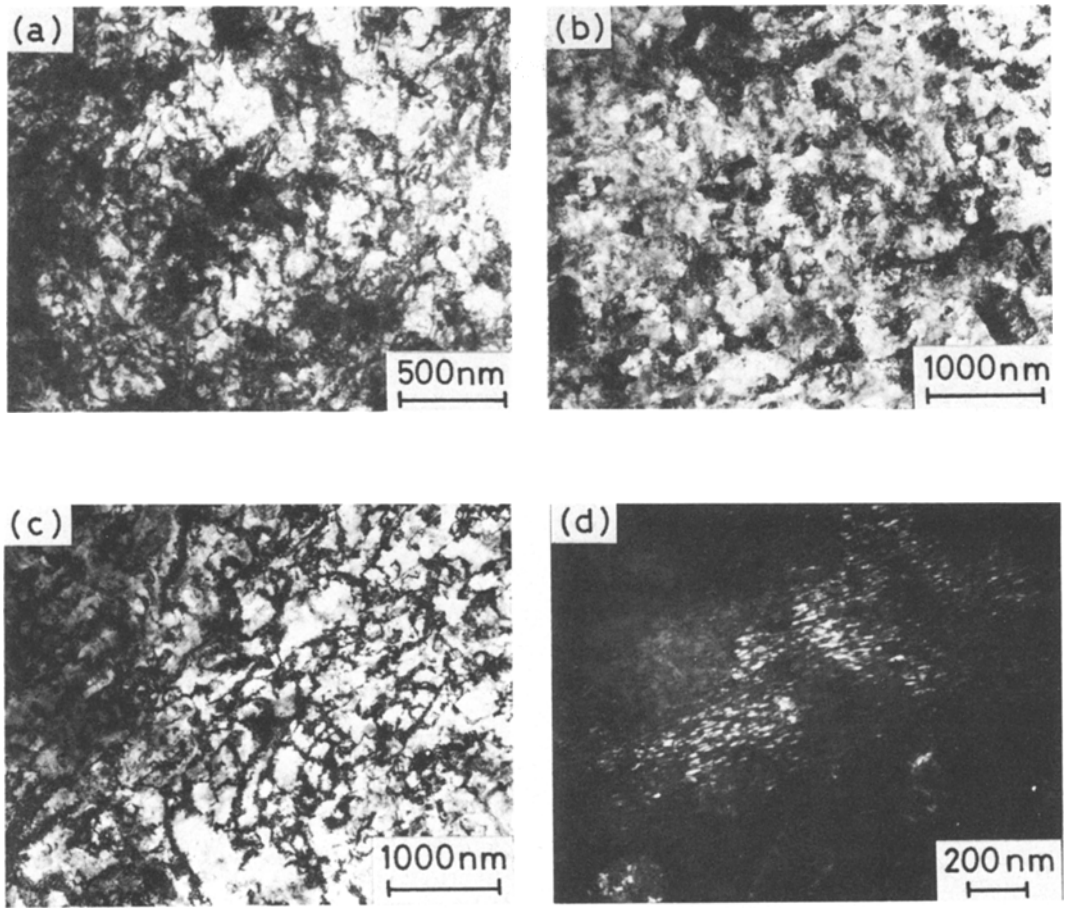

Figure 11 Bright-field micrograph in (a) the AW sample, (b) AWA sample, and (c) the AWAW sample. (d) Dark-field micrograph of ω in the AWAWA sample. Ageing at 623 k for 173×10^3 sec.

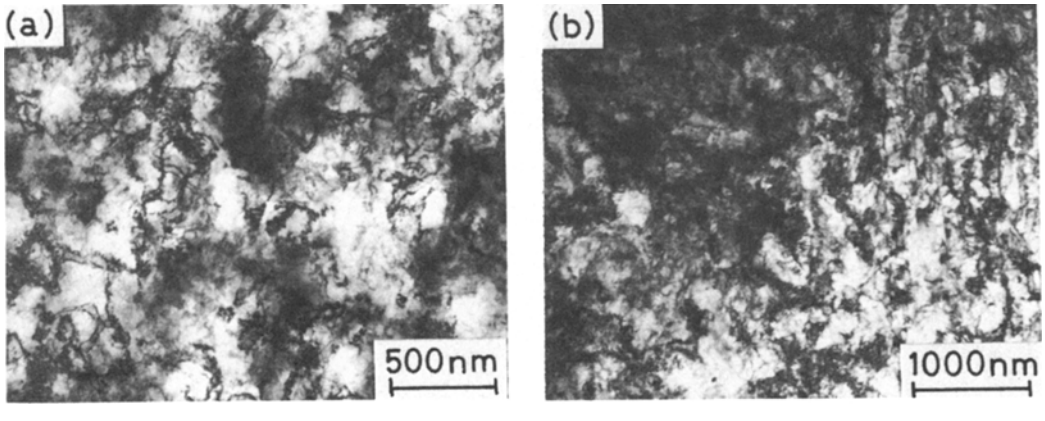

Figure 12 Bright-field micrograph in (a) the AW sample, (b) the AWA sample, (c) the AWAW sample, and (d) the AWAWA sample. Ageing at 673 K for 3.6×10^3 sec.

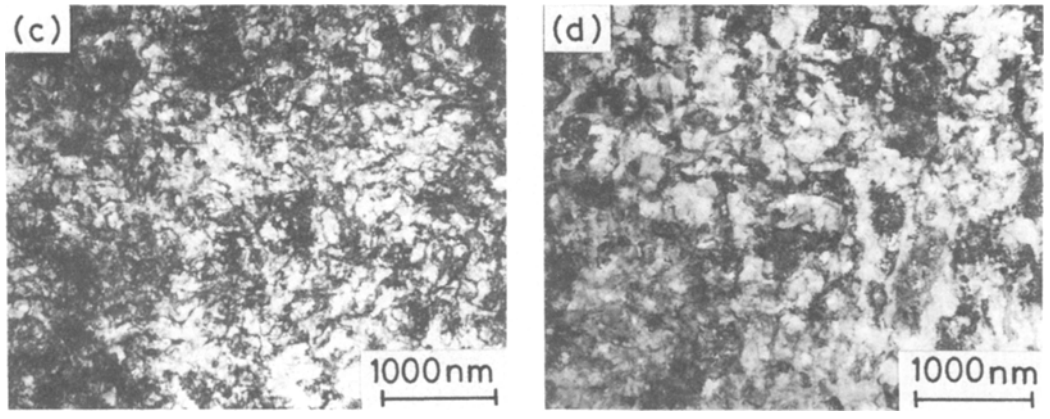

Figure 12 Continued

References

1. I. PFEIFFER and H. HILLMAN, *Acta Metall.* **16** (1968) 1429.
2. J. WILLBRAND and W. SCHLUMP, *Z. Metallkd.* **66** (1975) 714.
3. H. HILLMANN and K. J. BEST, *IEEE Trans. Mag.* **MAG-13** (1977) 1568.
4. K. J. BEST, D. GENEVEY, H. HILLMANN, L. KREMPASKY, M. POLAK and B. TRUCK, *ibid.* **MAG-15** (1979) 395.
5. S. A. ALTEROVITZ, J. A. WOOLLAM and E. W. COLLINGS, *ibid.* **MAG-15** (1979) 404.
6. K. J. BEST, D. GENEVEY, H. HILLMAN, L. KREMPASKY, M. POLAK and B. TURCK, *ibid.* **MAG-15** (1979) 765.
7. H. R. SEGAL, K. HEMACHALAM, T. A. DE WINTER and Z. J. J. STEKLY, *ibid.* **MAG-15** (1979) 807.
8. G. RONDELLI, E. OLZI and F. GHERARDI, *Z. Metallkd.* **71** (1980) 461.
9. F. ISHIDA, K. MATSUURA and T. DOI, *J. Japan Inst. Metals* **42** (1978) 217.
10. K. OSAMURA, E. MATSUBARA, T. MIYATANI, Y. MURAKAMI, T. HORIUCHI and Y. MONJU, *Phil. Mag.* **42** (1980) 575.
11. A. NAGATA, S. HANADA, S. DEN and O. IZUMI, "Titanium '80 Science and Technology", edited by H. Kimura and O. Izumi (AIME, New York, 1980) p. 755.
12. A. W. WEST and D. C. LARBALESTIER, *Adv. Cryogenic Eng.* **26** (1980) p. 471.
13. *Idem, IEEE Trans. Mag.* **MAG-17** (1981) 65.
14. *Idem, ibid.* **MAG-19** (1983) 548.
15. S. V. SUDAREVA, N. N. BUYNOV, V. A. VOZIL'KIN and M. I. BYCHKOVA, *Fiz. Met. Metalloved.* **29** (1970) 87.
16. D. C. LARBALESTIER, "Superconductor Materials Science", edited by S. Foner and B. B. Schwartz (Plenum Press, New York, 1981) p. 133.
17. B. S. HICKMAN, *Trans. Met. Soc. AIME* **245** (1969) 1329.
18. J. C. WILLIAMS, D. DE FONTAINE and N. E. PATON, *Met. Trans.* **4** (1973) 2701.
19. S. HANADA, A. TAKEMURA and O. IZUMI, unpublished research (1981).
20. S. HANADA, M. OZEKI and O. IZUMI, unpublished research (1983).
21. C. G. RHODES and J. C. WILLIAMS, *Met. Trans.* **6A** (1975) 2103.
22. C. G. RHODES and N. E. PATON, *ibid.* **8A** (1977) 1749.
23. T. J. HEADLEY and H. J. PACK, *ibid.* **10A** (1979) 909.
24. G. C. MORGAN and C. HAMMOND, "Titanium '80 Science and Technology", edited by H. Kimura and O. Izumi (AIME, New York, 1980) p. 1443.
25. S. HANADA and O. IZUMI, *Trans. Jap. Inst. Metals* **21** (1980) 201.
26. J. R. TORAN and R. R. BIEDERMAN, "Titanium '80 Science and Technology", edited by H. Kimura and O. Izumi (AIME, New York, 1980) p. 1491.
27. A. NAGATA, S. HANADA, S. DEN and O. IZUMI, *J. Jap. Inst. Metals* **47** (1983) 343.

Received 23 September
and accepted 4 October 1983